

Pinned and unpinned step dynamics on vicinal silver (110) surfaces

G. A. Held, D. M. Goodstein, and R. M. Feenstra

IBM Thomas J. Watson Research Center, P.O. Box 218, Yorktown Heights, New York 10598

M. J. Ramstad, D. Y. Noh, and R. J. Birgeneau

Department of Physics and Research Laboratory of Electronics, Massachusetts Institute of Technology, Cambridge, Massachusetts 02139

(Received 28 April 1993)

We present x-ray scattering and scanning-tunneling-microscopy studies of Ag(110) vicinally miscut along the $[\bar{1}10]$ direction. For a clean surface miscut by 1° we find no evidence for phase separation. However, for an impurity concentration of order $\lesssim 0.001$ monolayer we find that the pinning of steps results in a phase separation into flat (110) terraces and densely stepped regions. With increasing temperature, the clean surface exhibits a rapid decrease in step-step correlations primarily along the [001] direction.

Step interactions play a central role in determining the equilibrium morphology of a crystalline surface. Different interactions are known to result in such diverse phenomena as step pairing, surface faceting, and surface roughening.¹⁻⁶ A small density of steps may be incorporated onto a metal surface by deliberately cutting the crystal at an angle slightly off from a high-symmetry direction. If the high-symmetry surface does not reconstruct, the theory of equilibrium crystal shapes (ECS) predicts that at low temperatures the steps should either cluster together or spread uniformly across the surface.⁷ In the former case, a "hill and valley" structure of densely stepped rough regions coexisting with flat, high-symmetry facets will result. The fraction of the surface comprised of flat facets should decrease with increasing temperature, falling to zero at some temperature below the roughening transition temperature of the facet. In the latter case, the surface is predicted to be rough at all temperatures. That is, entropically wandering steps should result in a logarithmic divergence of the mean-square height fluctuations as a function of lateral distance across the surface.⁸ X-ray scattering, low-energy-electron-diffraction (LEED) and atom scattering studies have reported surface roughening of numerous metal crystalline facets, including Cu(110),² Ag(110),³ Cu(113)⁴ and Ni(113).⁵ In addition, studies of vicinally miscut Cu(110) (Ref. 2) and Ag(110) (Ref. 9) have reported low-temperature surface phase separation into a hill and valley structure.

The situation for Ag(110) is, however, controversial. In 1987 Held *et al.*³ carried out a high-resolution x-ray scattering study of a vicinal Ag(110) surface using a crystal which had been inadvertently miscut by $\sim 0.5^\circ$; they interpreted their data on the basis of a roughening transition of the flat (110) facets at ~ 725 K. More recently, Robinson *et al.*⁹ have readdressed this problem using a Ag(110) crystal miscut by $\sim 0.2^\circ$. They assert that, in equilibrium, their 0.2° vicinal Ag(110) surface phase separates into flat (110) facets together with stepped regions for temperatures below 790 K and that a uniform

step structure is only stable above that temperature. In order to resolve this controversy and indeed to understand generally the behavior of stepped Ag(110) surfaces we have carried out x-ray scattering and scanning-tunneling-microscopy (STM) studies of a Ag(110) sample miscut 1° from the [110] axis along the $[\bar{1}10]$ direction. For a clean and well-annealed surface, we find that at all temperatures above 300 K the surface is comprised of a uniform density of single atomic height meandering steps. That is, we find no evidence for vicinal phase separation. However, as the surface is annealed to sufficiently high temperatures, we find that impurities are driven to the surface and that this, in turn, results in the formation of large, flat (110) terraces. The latter is the behavior reported in Ref. 9 although they interpreted their data assuming a clean surface. For the clean surface we observe diffraction characteristic of uniform, albeit meandering, steps at all temperatures between 300 and 875 K. With increasing temperature, the step peaks lose intensity and undergo an evolution in line shape consistent with a decrease in step-step correlations, most noticeably in the [001] direction. While our data above 670 K are consistent with a rough surface, the peak evolution is not consistent with the simplest model of entropically repulsive steps, as discussed below.

The sample studied was mechanically polished and etched, with a resulting surface normal of 1° off the [110] axis along the $[\bar{1}10]$ direction. The sample was then mounted in an ultrahigh vacuum chamber and cleaned by repeated cycles of Ar-ion sputtering and thermal annealing. During the scattering experiments, the orientation of the samples was controlled by a two-tilt Huber diffractometer which was coupled to the chamber by means of bellows and a differentially pumped rotary seal. The chamber was equipped with LEED, Auger, and ion-sputtering capabilities; the base pressure was less than 1×10^{-10} torr. Details will be presented elsewhere. The scattering measurements were taken at the IBM/MIT beamline X-20A at the National Synchrotron Light Source. A beam of 9.5-keV photons was focused onto the

sample; the transverse resolution within the scattering plane was about $5 \times 10^{-5} \text{ \AA}^{-1}$ half-width at half maximum (HWHM). The resolution in the 2θ direction was set by slits at 0.085° HWHM.

Scattering from the clean 1° miscut surface is shown in Fig. 1. The final cleaning of this sample consisted of Ar-ion sputtering followed by annealing to 800 K for one-half hour. Figure 1(a) shows scattering through the $(0.98 \ 1.02 \ 0)$ position¹⁰ along the $(1\bar{1}0)$ direction—that is, along the miscut direction. Scattering from large (110) terraces would be precisely along the $(\bar{1}+Q_x, 1+Q_x, 0)$ rod. By contrast, large stepped regions yield diffuse rods of scattering passing through bulk peaks and inclined in the direction of the surface normal^{2,9} of the stepped region. The two peaks in Fig. 1(a) are cross sections of diffuse rods passing through the $(0 \ 2 \ 0)$ and $(\bar{2} \ 0 \ 0)$ bulk peaks and inclined towards the large stepped regions of the surface. Equivalently, the peaks can be viewed as arising from diffraction from the grating defined by the steps with the successive regions between the steps being 180° out of phase. The separation of these peaks corresponds to stepped regions inclined 0.95° from the $[110]$ axis along the $[\bar{1}10]$ direction, in good agreement with optical measurements of the macroscopic miscut. These measurements indicate that this surface is dominated by large, uniformly stepped regions oriented along the macroscopic miscut.

In Fig. 2(a) we plot scattering data at the $(0.05 \ 0.05 \ \bar{1})$ position¹⁰ along the $(1\bar{1}0)$ direction. This is the same sample discussed above only in this instance it has been prepared by annealing to 875 K for 4 h before cooling to 373 K. In addition to the two peaks corresponding to scattering from the stepped regions of the surface, there is now a dominant central peak at the $(0.05 \ 0.05 \ \bar{1})$ position, corresponding to scattering from large, flat (110) terraces.¹¹ Following collection of these data, the sample was Ar-ion sputtered at room temperature; the central

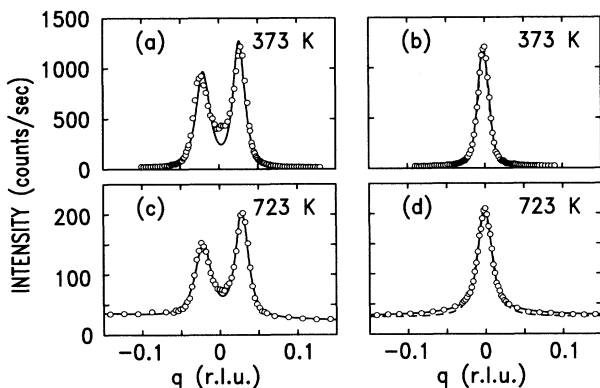


FIG. 1. Scans of the stepped surface peaks of a clean Ag(110) surface miscut 0.95° in the $[\bar{1}10]$ direction at the $(0.98 \ 1.02 \ 0)$ position at 373 and 723 K. (a) and (c) are scans along the $(1\bar{1}0)$ miscut direction while (b) and (d) are along (001) (transverse to the miscut), through the centers of the peaks at positive q in (a) and (c), respectively. The momentum transfer q measures the displacement in reciprocal-lattice units ($\text{rlu} \equiv 2\pi/a_0$) from $(0.98 \ 1.02 \ 0)$ in (a) and (c) and from the peak centers in (b) and (d).

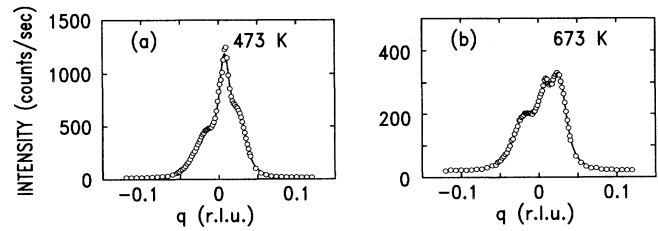


FIG. 2. Scans of the $(0.05 \ 0.05 \ \bar{1})$ surface peak position of a Ag(110) crystal miscut 0.95° along the $[\bar{1}10]$ direction at (a) 473 K and (b) 673 K after a 4-h anneal at 873 K. Scattering from both impurity pinned terraces (central peaks) and stepped regions of the surface (shoulders on the peaks) may be observed. The momentum transfer q measures the displacement in rlu from $(0.05 \ 0.05 \ \bar{1})$ along the $(1\bar{1}0)$ miscut direction.

terrace peak was observed to remain. However, after annealing to 800 K for one-half hour and then cooling to 373 K, data similar to those of Fig. 1(a) were recorded. This suggests that at 800 K the steps on a “clean” surface have sufficient mobility to rearrange themselves to an equilibrium configuration, without a significant density of step pinning impurities diffusing from the bulk of the crystal to the surface.

The separation of the step peaks in Fig. 2(a) corresponds to a stepped region inclined by 0.9° , approximately the macroscopic miscut of the entire surface. This indicates that although the central terrace peak is the dominant feature in Fig. 2(a), only a small fraction of the surface is in fact comprised of flat terraces. This conclusion is further supported by our observation of a strong dependence of the relative intensities of the step and terrace peaks on the out-of-plane momentum transfer. Specifically, the ratio of the integrated intensities of the sum of the step peaks to the terrace peak¹² in Fig. 2(a) is ~ 3.2 . If both the stepped and terrace regions were smooth we could conclude that 24% of the surface was comprised of flat terraces. However, we find that this ratio decreases rapidly as one moves from the out-of-plane $(1\bar{1}\bar{1})$ bulk peak to the $(0\ 0\ \bar{1})$ in-plane position, suggesting that the large relative intensity of the terrace peak at $(0.05 \ 0.05 \ \bar{1})$ results from the stepped regions being rougher than the terraced regions of the surface.¹³

With increasing temperature, the intensity of the terrace peak is observed to drop much more quickly than that of the step peaks; by 673 K the terrace and step peaks have comparable peak intensities [Fig. 2(b)] and by 775 K the terrace peak cannot be resolved above the step peaks. Since we cannot resolve any change in the positions of the step peaks from those corresponding to the macroscopic miscut angle, we cannot determine whether, with increasing temperature, the steps become unpinned and the terraces thus vanish, or alternately, the terraces remain intact but undergo a roughening transition near 725 K. Further diffraction studies of clean, extremely flat Ag(110) surfaces will be required to resolve this question.

The role of step pinning by impurities in the phase separation of vicinal Ag(110) is further demonstrated by imaging with STM a Ag(110) crystal with a 0.6° miscut. One such image of a $7000 \times 7000 \text{-\AA}^2$ region of the surface is shown in Fig. 3. The gray scale in the image is keyed

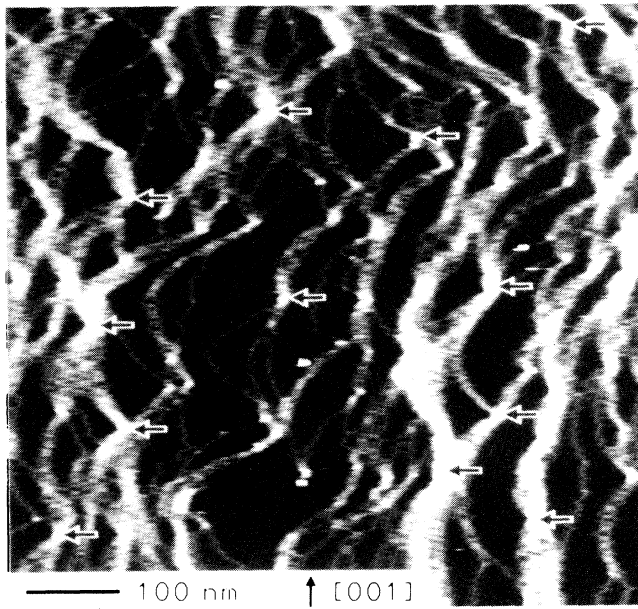


FIG. 3. STM image of the surface of Ag(110) crystal miscut 0.6° along the $[\bar{1}10]$ direction acquired at room temperature with a constant tunnel current of 1 nA and sample bias voltage of 1.5 V. The gray scale is keyed to a surface derivative computed along the horizontal direction. Monatomic steps appear as individual gray lines, and step bunches appear brighter. The step bunches are pinned by contamination clusters; some of the clusters are indicated by the arrows.

to a surface derivative computed in the horizontal direction; the individual gray lines in the image correspond to monatomic steps on the surface, and step bunches appear as brighter regions. Both large flat terraces and densely stepped regions are readily observable in the STM image. However, near the perimeter of almost every flat terrace one finds an impurity site at which a large number of steps are pinned, as indicated by the arrows in Fig. 3. These pinning centers appear to consist typically of a small cluster containing 10–20 impurity atoms. Dislocations are also observed to act as pinning sites, although they are found much less frequently than impurity clusters. Scanning many regions of the surface, we only observed phase separation in the presence of pinning sites, suggesting that this is indeed the mechanism for phase separation of vicinally miscut Ag(110) surfaces. The pointed structure of the step clusters near many of the pinning sites is similar to that observed to result from step flow due to evaporation from pinned steps on Si(100).¹⁴

We estimate the density of impurity sites in Fig. 3 to be of order 0.001 monolayer (ML). Similarly, after annealing our 1° miscut sample at 775 K for 48 h or 850 K for 4 h, no impurities could be observed by CMA Auger spectroscopy. However, after annealing to 875 K for 24 h, approximately 0.02 ML of sulfur was observed to have diffused to the surface. These observations show that levels of impurities which are undetectable by conventional Auger analysis are sufficient to alter radically the morphology of the surface.

The behavior reported in Ref. 9 for a nominally clean surface miscut 0.2° along an azimuth 30° from the $[\bar{1}10]$ axis is similar to our results for impurity pinned steps on 1° and 0.6° miscut surfaces. We cannot exclude the possibility that the sample studied in Ref. 9 was impurity free and did indeed exhibit phase separation below 790 K as the result of intrinsic step-step interactions. However, as we find with STM that the surface of a clean 0.6° miscut sample does not phase separate at any temperature above 300 K, this would require an extremely sensitive dependence of the phase-separation transition temperature on the step spacing (> 490 K per 0.4° of miscut). The observation that the steps in Fig. 3 appear qualitatively similar when meandering along the $[001]$ and $[\bar{1}10]$ directions suggests that the 30° difference in the azimuthal orientation between the miscut of our sample and that of Ref. 9 does not account for the significant differences in behavior observed. Also, we note that the annealing parameters cited in Ref. 9 are comparable to those with which we obtained an impurity pinned surface. Finally, the 0.2° miscut sample of Ref. 9 phase separates at nearly the same temperature as does our impurity pinned 1° miscut surface, suggesting that the same mechanism (such as step depinning) is occurring in each instance.

We now address the temperature dependence of the clean surface. In Figs. 1(a) and 1(c) we plot scans along the $(1\bar{1}0)$ direction of the $(0.98\ 1.02\ 0)$ position at 373 and 723 K, respectively. Figures 1(b) and 1(d) show scans along the (001) direction through the lower wave vector [positive q in Figs. 1(a) and 1(c)] step peak at these same temperatures. With increasing temperature, scans in the (001) direction undergo a loss of intensity and a marked decrease in peak-to-tail intensity ratio. The solid and dotted lines in Figs. 1(b) and 1(d) are best fits to a Kummer function and a Lorentzian to the 1.5 power ($L^{3/2}$), respectively. A Lorentzian to the 1.5 power corresponds to a model of finite-size domains with pure exponential correlations. A Kummer function $\Phi(1-\eta/2; 1; -q^2L^2/4\pi)$ has a Gaussian center portion of HWHM π/L and tails proportional to $1/q^{2-\eta}$, reducing to a Gaussian when η is equal to zero. Such a function describes the power-law scattering expected for a stepped surface in the presence of finite-size effects.¹⁵ Fitting our temperature series in the (001) direction to a Kummer function with the finite-size parameter L fixed at 267 Å, which is the 373-K best-fit value, we obtain the best-fit values of peak intensity and η shown in Figs. 4(a) and 4(b), respectively. The goodness-of-fit parameter χ^2 varies between 1.0 and 4.2 for these fits. Since vicinal Ag(110) is a two sublattice system, a simple Pokrovsky-Talapov¹⁶ model of meandering, entropically repulsive steps predicts power-law scattering with $\eta = \frac{1}{2}$, independent of temperature at the $(\bar{1}10)$ position. Our results shown in Fig. 4(b), however, imply that η increases progressively from ~ 0.4 at 373 K to ~ 1 at 850 K. This may be due either to direct nonentropic step-step interactions or to incipient roughening of the (110) terraces.

The lower-temperature data can also be reasonably fit by the $L^{3/2}$ form. The fitted values for the intensity and HWHM for this function are shown in Figs. 4(a) and 4(c). The goodness-of-fit parameter for these fits varies be-

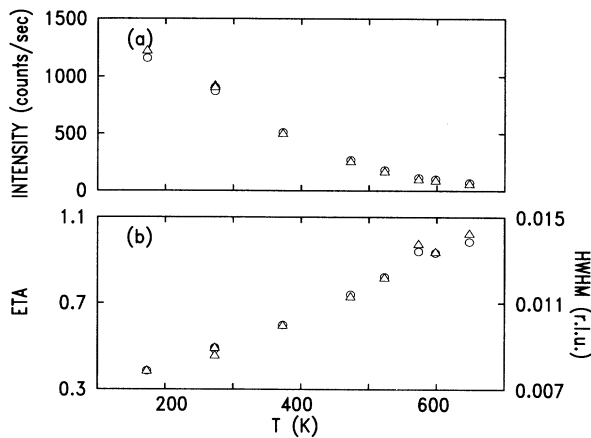


FIG. 4. (a) Peak intensity of the low wave-vector step peak near the $(0.98\ 1.02\ 0)$ position of the clean 0.95° miscut Ag(110) sample [positive q peak in Figs. 1(a) and 1(c)] as a function of temperature. Circles are fits of the scans along the (001) direction [Figs. 1(b) and 1(d)] to a Kummer function. Triangles are fits to a Lorentzian function to the 1.5 power (see text). (b) The exponent η from the Kummer fits (\circ) and the HWHM from the Lorentzian to the 1.5 power fits (\triangle) as functions of temperature.

tween 8 and 20, significantly worse than the corresponding Kummer function values. In these fits, the HWHM increases from 0.0076 to 0.0138 reciprocal-lattice units (rlu) between 373 and 848 K. As is evident in Fig. 1(d), above ~ 675 K the $L^{3/2}$ function underestimates the intensity in the tails, further demonstrating that the temperature evolution of this peak is primarily a change in peak-to-tail ratio and not simply a change in width.

As is evident in Figs. 1(a) and 1(c) the temperature evolution of the line shapes in the $(\bar{1}10)$ direction is much less pronounced. For example, when the data are fit to a $L^{3/2}$ line shape the widths of the step peaks increase by

less than 10%. The fact that this broadening is much less than that observed in the (001) direction is not unexpected; the addition of step kinks in the [001] direction requires only the breaking of next-nearest-neighbor bonds, whereas kinks in the $(\bar{1}10)$ direction require the breaking of nearest-neighbor bonds. Kummer function fits with η fixed at the values obtained from (001) scans, Figs. 1(b) and 1(d), and with the power-law length scale ratio held fixed at unity are unsatisfactory below 700 K. If the length scale ratio were allowed to float⁶ then presumably satisfactory fits could be obtained but the number of adjustable parameters would then be unreasonably large.

In summary, we find that the surface morphology of vicinal Ag(110) depends remarkably sensitively on the cleanliness of the surface. Small numbers of pinning centers cause steps to agglomerate for temperatures up to 750–800 K; this, in turn, produces large, flat (110) terraces. These results appear to resolve the discrepancies in interpretation between previous studies^{3,9} of vicinal Ag(110). It is notable that all three experiments find the scattering from flat (110) terraces to vanish above ~ 775 K. This suggests that either the true roughening transition of an ideal Ag(110) facet would occur around 775 K, or, alternately, the bound steps become unpinned above this temperature. For a nominally clean surface, however, our x-ray diffraction and STM data are consistent with uniformly spaced meandering monatomic steps. With increasing temperature these steps undergo a loss of positional correlations. However, the manner in which they do so is not consistent with a simple model of entropically repulsive steps.

We wish to thank W. Haag for technical assistance and J. Toner for helpful discussions. The MIT component of this research was supported by the Joint Services Electronics Program under Contract No. DAAL-03-89-C-0001.

¹X. Tong and P. A. Bennett, Phys. Rev. Lett. **67**, 101 (1991).
²S. G. J. Mochrie, Phys. Rev. Lett. **59**, 304 (1987); B. M. Ocko and S. G. J. Mochrie, Phys. Rev. B **38**, 7378 (1988).
³G. A. Held, J. L. Jordan-Sweet, P. M. Horn, A. Mak, and R. J. Birgeneau, Phys. Rev. Lett. **59**, 2075 (1987).
⁴K. S. Liang, E. B. Sirota, K. L. D'Amico, G. J. Hughes, and S. K. Sinha, Phys. Rev. Lett. **59**, 2447 (1987); B. Salanon, F. Fabre, J. Lapujoulade, and W. Seike, Phys. Rev. B **38**, 7385 (1988).
⁵E. H. Conrad, L. R. Allen, D. L. Blanchard, and T. Engel, Surf. Sci. **187**, 265 (1987); I. K. Robinson, E. H. Conrad, and D. S. Reed, J. Phys. (Paris) **51**, 103 (1990).
⁶R. J. Phaneuf and E. D. Williams, Phys. Rev. Lett. **58**, 2563 (1987); D. Y. Noh, K. I. Blum, M. J. Ramstad, and R. J. Birgeneau, Phys. Rev. B **44**, 10969 (1991).
⁷C. Herring, Phys. Rev. **82**, 87 (1951); for a review see C. Rottman and M. Wortis, Phys. Rep. **103**, 59 (1984).
⁸J. D. Weeks, in *Ordering in Strongly Fluctuating Condensed Matter Systems*, edited by T. Riste (Plenum, New York, 1980), p. 293; J. Villain, D. R. Grompel, and J. Lapujoulade, J. Phys. F **15**, 809 (1985).

⁹I. K. Robinson, E. Vileg, H. Hornis, and E. H. Conrad, Phys. Rev. Lett. **67**, 1890 (1991).

¹⁰Throughout the text we use bulk crystallographic notation. In the rectangular surface notation of LEED and Ref. 9: $(\bar{1}\bar{1}0)_{\text{bulk}} = (010)_{\text{surface}}$, $(001)_{\text{bulk}} = (100)_{\text{surface}}$, and $(110)_{\text{bulk}} = (001)_{\text{surface}}$. Thus, the $(0.98\ 1.02\ 0)_{\text{bulk}}$ position corresponds to the $(0\ \bar{1}\ 0.02)_{\text{surface}}$ position along the $(0\ \bar{1}\ Q_z)_{\text{surface}}$ diffraction rod, while $(0.05\ 0.05\ \bar{1})_{\text{bulk}}$ corresponds to $(\bar{1}\ 0\ 0.05)_{\text{surface}}$ along the $(\bar{1}\ 0\ Q_z)_{\text{surface}}$ diffraction rod.

¹¹From scans through the $(0.05\ 0.05\ \bar{1})$ peak, we estimate the (110) terraces to be on average 250 and 400 Å in the $[1\bar{1}0]$ and [001] directions, respectively, using the definition: domain size = π/HWHM .

¹²Integrated intensity is defined as peak intensity multiplied by the peak widths in the $(\bar{1}\bar{1}0)$ and (001) directions.

¹³I. K. Robinson, Phys. Rev. B **33**, 3830 (1988).

¹⁴M. Mundscha, E. Bauer, W. Telieps, and Swiech, Surf. Sci. **223**, 413 (1989).

¹⁵P. Dutta and S. K. Sinha, Phys. Rev. Lett. **47**, 50 (1981).

¹⁶V. L. Pokrovsky and A. L. Talapov, Phys. Rev. Lett. **42**, 65 (1979); H. J. Schulz, Phys. Rev. B **22**, 5274 (1982).

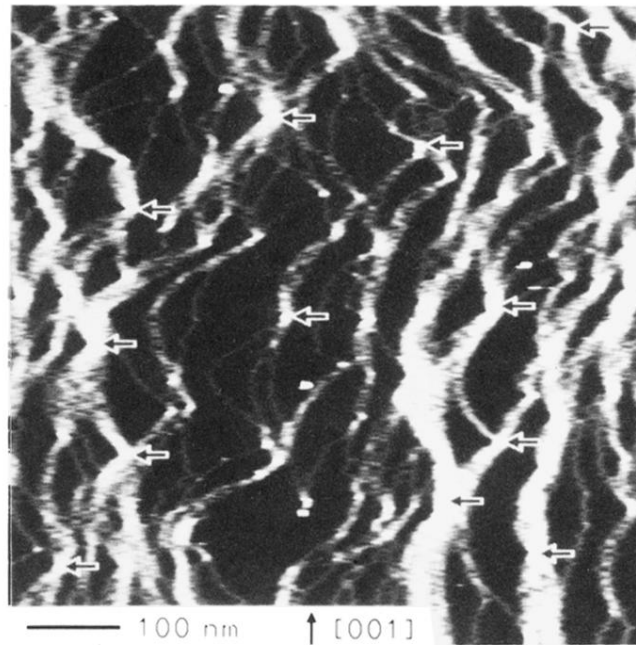


FIG. 3. STM image of the surface of Ag(110) crystal miscut 0.6° along the $[\bar{1}10]$ direction acquired at room temperature with a constant tunnel current of 1 nA and sample bias voltage of 1.5 V. The gray scale is keyed to a surface derivative computed along the horizontal direction. Monatomic steps appear as individual gray lines, and step bunches appear brighter. The step bunches are pinned by contamination clusters; some of the clusters are indicated by the arrows.